Aeroelastic Stability Analysis of a Wind Tunnel Wing Model Equipped with a True Scale Morphing Aileron

Francesco Rea, Rosario Pecora, Francesco Amoroso, Maurizio Arena, and Maria Chiara Noviello
Dept. of Industrial Engineering, University of Naples "Federico II", Naples, Italy
Email: francesco.rea@unina.it

Gianluca Amendola
Smart Structures Division, Italian Aerospace Research Centre (CIRA), Capua, CE, Italy

***Abstract*— In last decades, several research programs were founded worldwide to exploit the potentialities of the morphing concepts, especially to improve aerodynamic efficiency, and so reduce fuel consumption. Among these, the CRIAQ MDO-505 project represents the first joined research program between Canadian and Italian academies, research centers and leading industries. The aim of the project is to design, manufacture and tests in wind tunnel facilities a morphing wing tip for a Bombardier-type aircraft controlled by electric actuators and pressure sensors. In such framework, the authors intensively worked on the flutter clearance demonstration of the wind tunnel wing model equipped with a full-scale variable-camber aileron driven by load-bearing electro-mechanical actuators. Rational approaches were implemented in order to simulate the effects induced by variations of aileron actuator's stiffness on the aeroelastic behavior of the wing. Reliable models were properly implemented to enable fast aeroelastic analyses covering several configuration cases in order to prove clearance from any dynamic instability (flutter) up to 1.2 times the maximum flow speed expected during Wind Tunnel Tests. Finite-element models were properly developed in order to obtain and implement wing model modal parameters (modes shapes, frequencies, generalized masses, damping) in SANDY®, an in-house developed code, that was used for the definition of the coupled aero-structural model as well as for the solution of aeroelastic stability equations by means of theoretical modes association in frequency domain. Obtained results were finally arranged in a diagram showing trend of the flutter speed with respect to changes in control surface harmonic covering a wide range of values for the stiffness of the aileron (external) actuator.**

***Index Terms*—morphing aileron, aeroelasticity, flutter, aeroelastic stability, variable camber, active ribs, smart structures, FEM.**

I. Introduction

The conventional aircrafts wing can achieve the best performance only during the most important flight stage suggested by the mission that the aircraft must accomplish. Out of the most important flight stage, the aircraft performances are severely affected.

Therefore, the need of more performing wing has led designers to the concept of morphing so as to make the aircrafts able to adapt and optimize their shape to obtain the best performances in all flights conditions.

To fulfill specifications in dissimilar stages of the flight envelope, an aircraft usually uses aerodynamic devices (such as flaps, slats, etc.) to change the wing camber on specific parts (leading edge and trailing edge). However, morphing devices are used to change the overall wings camber to achieve the greater aerodynamic benefits. The morphing wings devices accomplish to several specific objectives: optimize take-off and landing performances by variable-camber flaps, aerodynamic flow control and drag reduction by overall variable-camber wing, aerodynamic load control by variable-camber trailing edge of the wing tip.

In the mid of 80s NASA and USAF proposed the Advanced Fighter Technology Integration (AFTI)/F-111 Mission Adaptive Wing (MAW) program whose purpose was to integrate, on board of military aircraft, an automated controlled device for wing camber morphing [1]. The automated control system was able to achieve several optimized conditions (maximized lift/ratio, maximized cruise speed at proper altitude, load control) basing on measurements of dynamic pressure, normal acceleration, Mach number. Flight test conducted on the AFTI/F-111 aircraft confirmed the expected performance improvement: 20% range enhancement, 20% aerodynamic efficiency growth, 15% increase of wing air load at constant bending moment [1].

Reducing fuel consumption has become a central concern around the world over the past few years, due to the detrimental environmental effects.

Research effort for the best solutions to reduce aircraft fuel consumption has therefore captured the attention of industry, academia and government institutions.

In the last decades [2], several research programs were founded worldwide to exploit the potentialities of the morphing concepts, especially to improve aerodynamic efficiency and so reduce fuel consumption.

Manuscript received June 24, 2017; revised October 12, 2017.

doi: 10.18178/ijmerr.6.6.440-450

Starting in 2011, Smart Intelligent Aircraft Structures (SARISTU) research project represents the largest European funded research project that focuses on the challenges posed by the physical integration of smart intelligent structural concepts on a CS-25 category aircraft. One of the SARISTU goals was to demonstrate the structural feasibility of individual conformal morphing concepts concerning the leading edge and the trailing edge on a full-scale outer wing section by aerodynamic and structural testing [3].

Within the framework of the JTI-Clean Sky project, Green Regional Aircraft "Low Noise Configuration" domain, design and technological demonstration of an innovative flap architecture for CS-25 category regional aircraft was provided [4].

Starting in 2013, the Consortium for Research and Innovation in Aerospace in Quebec (CRIAQ) Multidisciplinary Design Optimization (MDO) 505 project represents the first joined program between Canadian and Italian academies, research centers and leading industries.

Figure 1. Wing model equipped with morphing aileron [8].

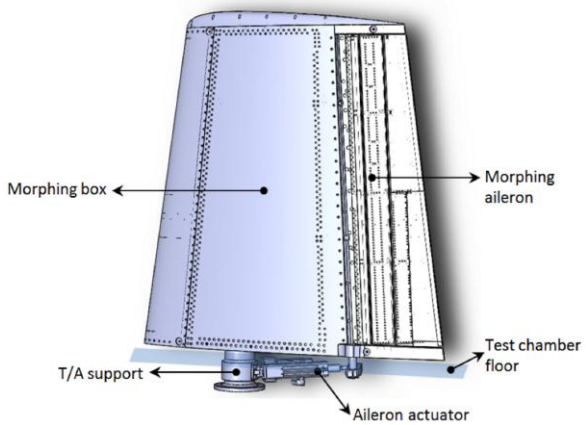

Figure 2. Test article (T/A) assembly.

The main objective of the teams working on the international (Italy-Canada) project was to design and manufacture and test in wind tunnel facilities a morphing wing tip for a Bombardier-type aircraft controlled by electric actuators and pressure sensors [5]. The main objective of the desired morphing behavior was to delay the flow transition on the wing; consequently, aerodynamic efficiency of the wing and aerodynamic performances of the aileron could be improved [6], [7].

Moreover, the program addresses the fulfillment of combined smart structures to improve wings efficiency: an adaptive-bump configuration for the upper skin of the wing box designed by the Canadian team, and a variable-camber aileron architecture designed by the Italian team.

The aerodynamic numerical results were validated by means of wind tunnel testing to be held at the Institute for Aerospace Research (IAR-NRC) Subsonic Wind Tunnel [8]. The wing model setup equipped with the morphing aileron installed in the wind tunnel test is shown in Fig. 1. The wing model 3D CAD mock-up (Fig. 2) shows that the aileron rotation around its hinge axis is assured by a linear actuator connected to a stiff cylindrical support holding the entire test article, constrained to the wind tunnel by means of bolts.

The linear actuator and the cylindrical support (Fig. 2) are both placed out of the test chamber and therefore not subjected to the aerodynamic flow. The wing-box, designed by the Canadian Team, has a conventional structural architecture equipped with a flexible composite skin on the upper surface of the dry area between spars, which will be morphed by a set of actuators [9]. The morphing aileron (designed by the Italian team) is made up of segmented adaptive ribs to achieve transition from baseline configuration to a desired target shape [10].

In order to assure the safety of Wind Tunnel Tests campaign, the aeroelastic behavior of the test article was investigated and clearance from any dynamic instability (flutter) was demonstrated up to 1.2 times the maximum flow speed expected during tests (85 m/s).

The present study, based on rational analysis inspired to potentially applicable airworthiness requirements, consisted of four consecutive main steps:

- Evaluation of test article (T/A) theoretical modes (with reference to the constraints condition to be reproduced during the Wind Tunnel Tests);
- Generation of test article aerodynamic lattice;
- Interpolation of modes on aerodynamic lattice and Generalized Aerodynamic Force (GAF) evaluation;
- Flutter analysis by theoretical modes association.

In-depth analysis of the aeroelastic behavior was performed. Investigation of the variable-camber morphing modal behavior coupling with bending and torsional wing section modes was fully provided.

Finally, a sensitivity analysis of the external linear actuator stiffness on the aeroelastic behavior of the test article was defined in order to prove robustness of the obtained results with respect to changes in control surface harmonic.

The structural model of the test article was generated in MSC-PATRAN® environment and processed by MD-NASTRAN® according to sol. 103 protocol [11].

All the actions related to the aeroelastic analysis were carried out using SANDY-software facilities; a short description of its principal characteristics (and validation cases) has been therefore provided in Appendix.

II. Morphing Aileron Architecture

The morphing aileron device was designed in order to enable the controlled transition of wing trailing edge airfoil from a baseline configuration to predefined targets shapes with continuous monotonic camber and no elongation in chord.

Such target shapes are matched by a tailored kinematics driven by an appropriate actuation system.

The aileron airfoil was then approximated by a segmented rib architecture based on a finger-like layout properly tailored to enable aileron camber morphing upon actuation.

Each rib (Fig. 3) was assumed to be segmented into three consecutive blocks (B1, B2 and B3) connected by means of hinges located on the airfoil camber line (A, B). Block B1 is rigidly connected to the rest of the wing structure through a torsion tube enabling aileron rotation for roll control. Blocks B2 and B3 are free to rotate around the hinges on the camber line, thus physically turning the camber line into an articulated chain of consecutive segments.

A linking rod element (L) hinged on non-adjacent blocks forces the camber line segments to rotate according to specific gear ratios.

The linking element makes each rib equivalent to a single-DOF mechanism: if the rotation of any of the blocks is prevented, no change in camber/shape can be obtained; on the other hand, if an actuator moves any of the blocks, all the other blocks follow the movement accordingly.

The rib mechanism therefore uses a three-segment polygonal line to approximate the camber of the airfoil and to morph it into the desired configuration while keeping the airfoil thickness distribution unchanged [10].

The ribs' kinematic is transferred to the overall aileron structure by means of a multi-box arrangement (Fig. 4). Each box of the structural arrangement is characterized by a single-cell configuration delimited along the span by homologue blocks of consecutive ribs, and along the chord by longitudinal stiffening elements (spars and/or stringers).

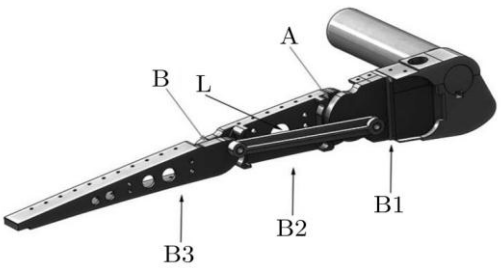

Figure 3. Morphing rib architecture.

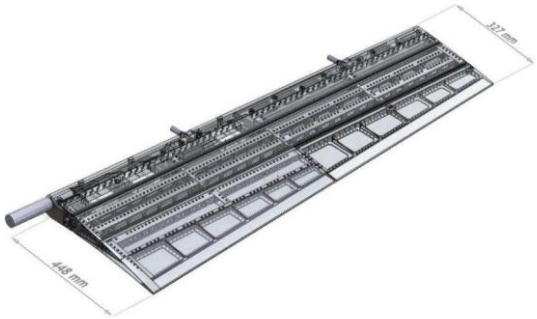

Figure 4. Morphing aileron: multi-box arrangement.

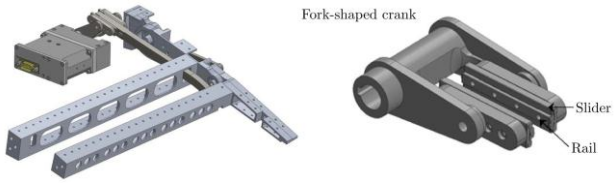

Figure 5. Morphing aileron deflections: (a) down, (b) up.

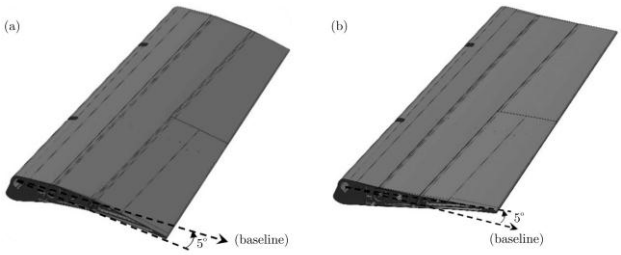

Figure 6. Actuation system and rib.

Upon the actuation of the ribs, all the boxes are put into movement, thus changing the external shape of the aileron; if the rotation of any rib blocks is prevented by locking the actuation chain, the multi-box structure is elastically stable under the action of external aerodynamic loads. A four-bay (five-rib) layout was considered for an overall (true-scale) span of 1.4m; AL2024-T351 alloy was used for spars, stringers and rib plates, while C50 steel was used for the ribs' links [10]. The external structure is made up of segmented aluminum-alloy skin embedding standard gap-filler, as shown in Fig. 5.

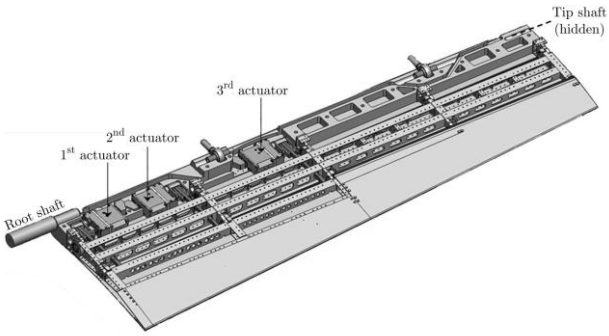

Figure 7. CAD of the morphing aileron: internal view.

The ribs' kinematic is based on a oscillating glyph mechanism which transforms the actuator shaft rotation into a rib deflection by means of a leverage directly linked to the rib plate.
This mechanism has been theoretically studied in [12], [13] and it has the advantage to exhibit an increasing torque amplification factor as the rib-morphing angle rises [13]. Further details on the actuation system are shown in Fig. 6. Finally, the morphing aileron is connected to the wing model by means of root and tip shaft as shown in the Fig. 7.

III. Wind-Tunnel Test Article Aeroelastic Model

The Wind-Tunnel Test (WTT) article aeroelastic model was generated according to a rational analysis inspired to potentially applicable airworthiness requirements [14].

The main steps defined were: evaluation of test article modal parameters, generation of test article aerodynamic lattice, and interpolation of modes on aerodynamic lattice and Generalized Aerodynamic Forces (GAF) evaluation. The aeroelastic model was used to solve the dynamic aeroelastic equation by adopting PK-continuation method [15] and modal frequency/damping trends versus airflow speed were traced in order to detect potential static and dynamic instabilities.

As first step, the finite-element (FE) model was generated in order to evaluate test article (T/A) modal parameters with reference to constraint conditions expected during Wind Tunnel Tests (WTT).

As second step, test article (T/A) main geometrical data were obtained by CAD assembly, and used for generation of wing model aerodynamic lattice; in addition, matrices of unsteady Aerodynamic Influence Coefficients (AIC) were evaluated by means of Doublet Lattice Method (DLM)[15].

Finally, displacements induced by elastic modes along the normal of each aerodynamic box, were obtained through surface spline interpolation of modal displacements exhibited by selected grid points. All tasks, related to the three main steps, were carried out using SANDY®-software facilities. Further details, about each step, will be outlined below.

A. Structural Model

The structural model of the aileron was assembled into the finite-element (FE) model of the wing box suitably generated in order to evaluate the normal modes of the entire test article (T/A). The hinged connection between the aileron and the wing box was accurately reproduced as well as the mechanical system for the actuation of the control surface.

Wing box geometry [9] was simplified and adjusted in order to achieve high mesh quality. A general overview of the wing box mesh is provided by Fig. 8; adopted materials properties and elements summary are respectively reported in Table I and Table III. As reported in Table I, the external actuator was modeled through a rod element linked to the test article (T/A) support and to the lever arm of the aileron hinge axis (Fig. 9).

Four different values for the linear stiffness of the actuator were taken in account (Table II) in order to assess the aeroelastic stability of the test article with respect to changes in control surface harmonics. Actuator stiffness was modified by working on the Young modulus of the rod element (CROD, [16]) according to the following equation:

$$E = K*L/A \quad (1)$$

where:

- L is the length of the actuation rod simulating the actuator;
- A is the section of the actuation rod simulating the actuator;
- K is the value assigned to the actuator stiffness.

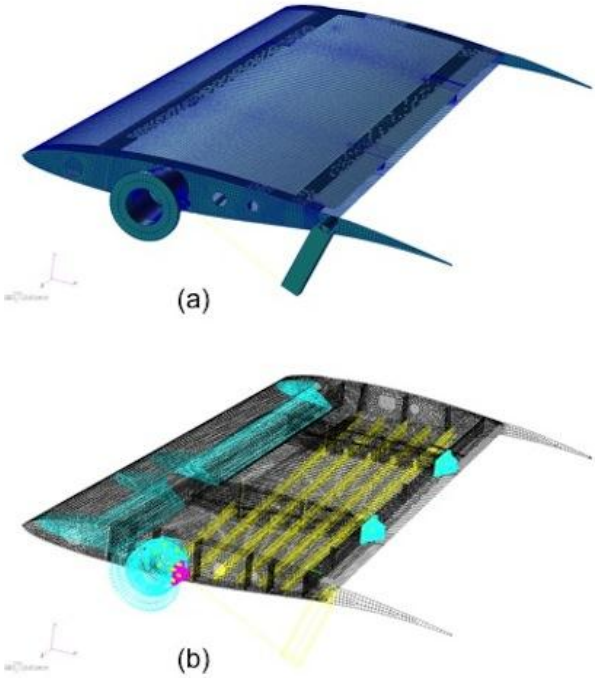

Figure 8. Wing box: (a) complete model, (b) wireframe view.

TABLE I. Wing-Box (FE) model: Material Properties.

MAT. (ISOTR.)	E [GPa]	ρ [Kg/m³]	ν	REFERENCE ITEM	
Harmonic Steel	210	7850	30	T/A support, hinge blocks, lever arm (ext. actuator)	
Al2024-T351	70	2768	0.33	All wing box items (except the upper skin)	
Fiberglass Renshape 5020	9.48	160.18	0.22	Leading edge core	
MAT. (ORTH.)	**E_1 [GPa]**	**E_2 [GPa]**	**G_{12} [GPa]**	**ρ [Kg/m³]**	**REFERENCE ITEM**
Laminate	63.7	49.9	16.5	1600	Upper skin panel

TABLE II. WING-BOX (FE) MODEL: ELEMENTS SUMMARY.

ELEMENT TYPE	NUMBER ELEM.	REFERENCE ITEM
CBEAM	475	Morphing skin actuators; Joints between the root rib T/A support
CROD	1	External actuator (for aileron rigid deflection)
CQUAD4	39563	Skin
CTRIA3	64	Skin
CHEXA	29933	Leading edge core and T/A support
RBE2	14	Joints between the root rib and the T/A support; joints between morphing skin actuators and surrounding structure

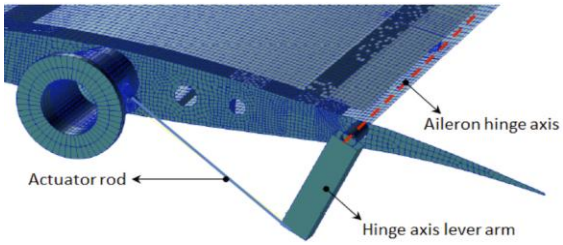

Figure 9. Actuator model (actuator rod).

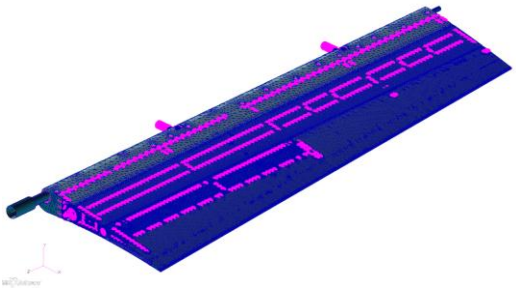

Figure 10. Morphing Aileron Finite element (FE) model.

Modal analysis in absence of actuator rod connection was preliminary carried out and FE modal capability to reproduce aileron fundamental (rigid mode, 0Hz, reproducing aileron rotation around its hinge axis) was positively checked.

For all the analysis reported, the test article (T/A) support (Fig. 2) was constrained coherently with the bolted connection to the with tunnel floor (Fig. 2). Indeed, the complete FE model was generated assembling:

- FE model of the wind tunnel wing box (Fig. 8) tailored for assessment of its dynamic behavior;
- FE model of the morphing aileron (Fig. 10) characterized by refined mesh specifically conceived for detailed stress analysis (further detail on the model in [13]) and properly updated by means of Ground Vibration Test (GVT)[17].

The complete test article finite-element model was generated in MSC-PATRAN®, and real eigenvalue extraction was performed, according to MSC-NASTRAN® SOL 103 protocol [16], by means of Lanczos Method in the frequency range of interest ([0 Hz; 80 Hz]) with eigenvectors normalized to the maximum value [16].

As first step, before aeroelastic analysis results, the modal database for several external actuator stiffness values was analyzed. The first modal shape (Fig. 11) shows aileron harmonic (i.e. frequency of the elastic deflection at locked actuators). Concerning the first mode (*aileron harmonic*) modal frequency increases, as external linear actuator stiffness increases, due to the higher torsional stiffness on the aileron shaft; on the other hand, modal shape remains mostly the same.

The second modal shape (Fig. 12) shows entire test article in plane bending due to support stiffness. Regarding the second mode (*T/A bending mode*) modal frequency and shape remain almost the same, as the external linear actuator stiffness increases, because they are not affected by the external actuator stiffness.

The third mode (*aileron tab mode* Fig. 13) shows wing bending, due to the test article support stiffness, plus chord-wise bending of two last aileron blocks.

The external linear actuator stiffness does not affect frequency and shape of the third mode, which remain almost the same. The fourth mode (Fig.14) shows morphing aileron elastic deformation due to the stiffness of its actuation system.

TABLE III. ACTUATOR STIFFNESS.

K [N/m]	E [N/m^2]
5.0 E+04	6.80 E+06
1.0 E+05	1.36 E+07
1.5 E+05	2.04 E+07
2.0 E+05	2.72 E+07

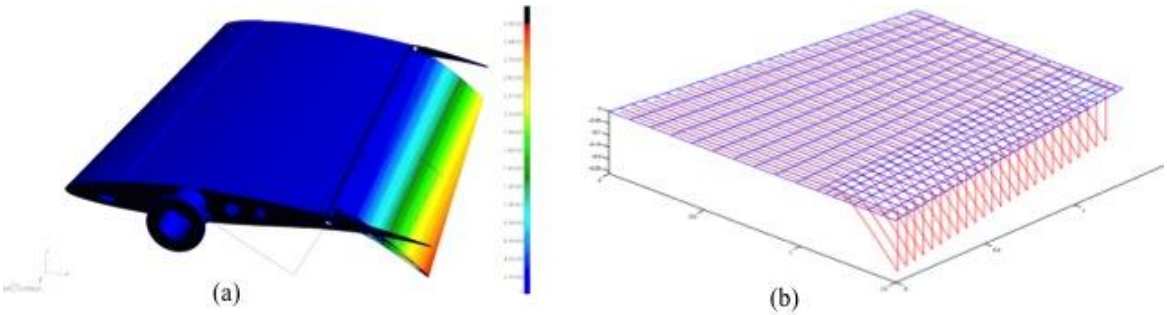

Figure 11. Aileron harmonic: (a) modal displacements on structural model, (b) interpolated displacements on aero-lattice.

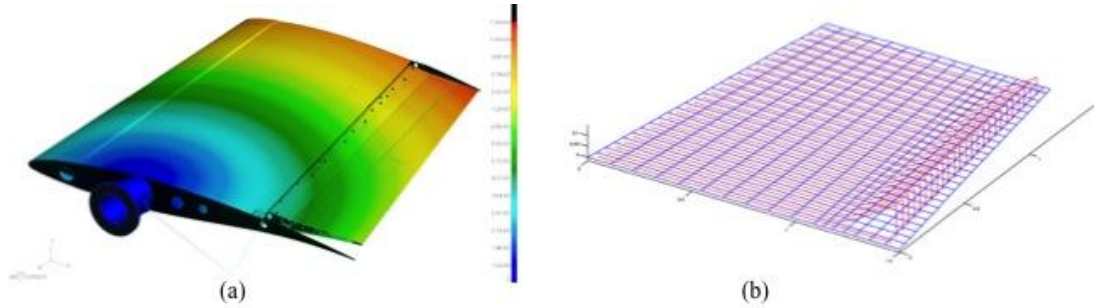

Figure 12. Test article (T/A) bending mode: (a) modal displacements on structural modal, (b) interpolated displacements on aero-lattice.

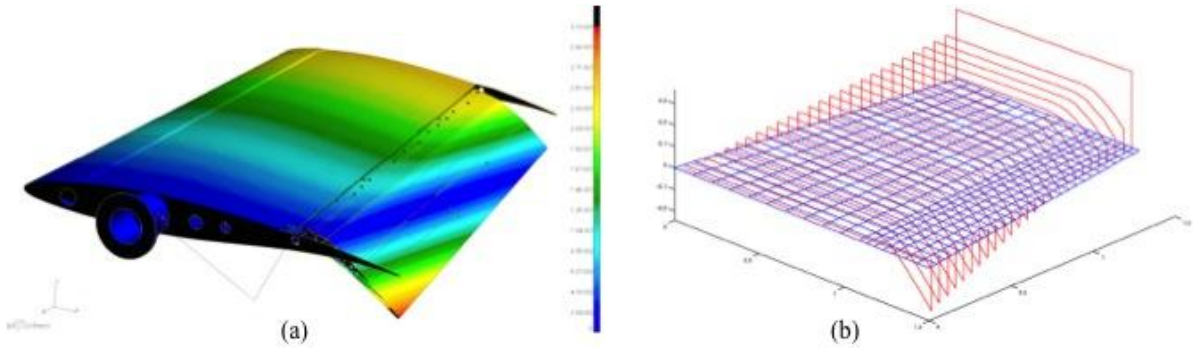

Figure 13. Aileron tab mode: (a) modal displacement on structural model, (b) interpolated displacements on aero-lattice.

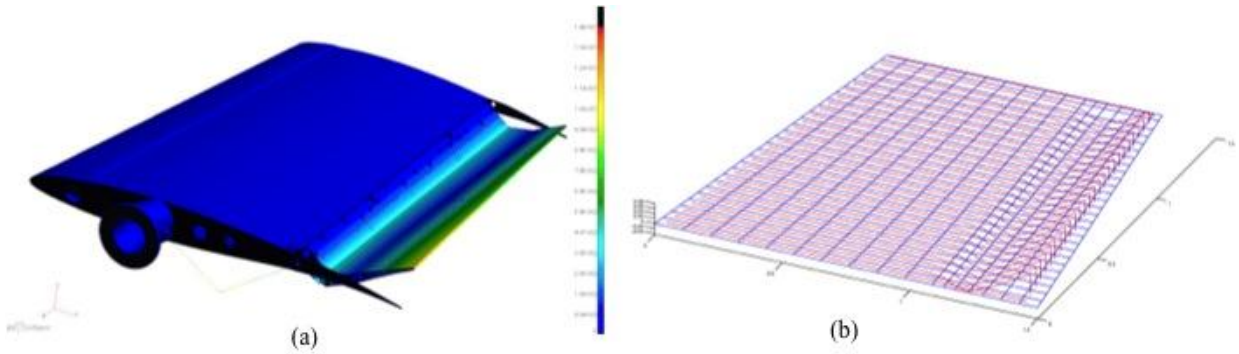

Figure 14. Fourth mode: (a) modal displacements on structural model, (b) interpolated displacement on aero-lattice.

In order to perform fast sensitivity analysis, a reduced number of FEM grids were selected from whose modal eigenvectors the complete modal database could be properly reconstructed. Indeed, FEM grids were located on forward and rear spar of the wing box in order to detect wing-box bending and torsion.

Several FEM grid points were selected on the segmented ribs of the morphing aileron: two on the first and second block, and three on the third block Fig.15a(/b). In such a way, aileron chord-wise bending and torsion modal shapes were effectively detected.

The entire set of grids used for modes interpolation has been marked in yellow (/red) in Fig. 15a(/b). Finally, the modal database (modes shapes, frequencies, generalized masses, damping) was used for the definition of the coupled aero-structural model.

B. Aerodynamic and Interpolation Model

The aerodynamic lattice of the morphing wing tip was generated by properly meshing the middle wing plane through four macro-panels; macro-panels were further meshed into elementary boxes; higher boxes density was considered for the morphing aileron and, to assure mesh uniformity also for the not-movable wing trailing edge.

The aerodynamic lattice has been sketched in Fig. 16. Six flat panels characterized the aerodynamic lattice:

- Three panels for the wing box: P1 (inner wing region), P2 (mid wing region), P3 (outer wing region);
- Three panels for the morphing aileron: P4-P6 (one for each moveable segment).

Each aerodynamic panel was rationally meshed into strips and elementary boxes. Panels' boundaries (Fig. 16) have been represented by bold lines while the boxes pertinent to the aileron have been filled with gray color.

Displacements induced by elastic modes along normal of each aerodynamic box, were obtained through surface spline interpolation of the modal displacements at the selected FEM grids.

The entire set of grids used for modes interpolation has been marked in yellow (/red) in Fig. 15a (/b).

The aerodynamic lattice was useful to evaluate the unsteady Aerodynamic Influence Coefficients (AIC) matrices, by means of Doublet Lattice Method (DLM), for specific values of reduced frequencies.

Roger's Rational Function Approximation (RFA) method was used to interpolate unsteady Aerodynamic Influence Coefficient (AIC) at definite values of reduced frequencies requested in iteration process of PK-Continuation method [15].

Finally, displacements interpolated on the aerodynamic lattice (Fig. 11a) properly matched modal displacements on the structural model (Fig. 11b).

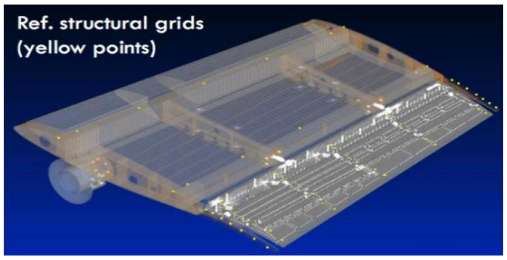

(a)

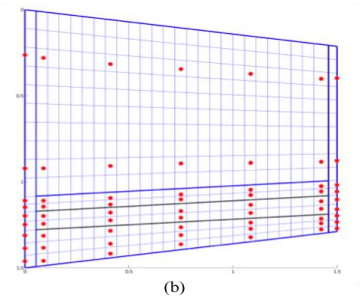

(b)

Figure 15. Interpolation grids on (a)structural and (b) aerodynamic model.

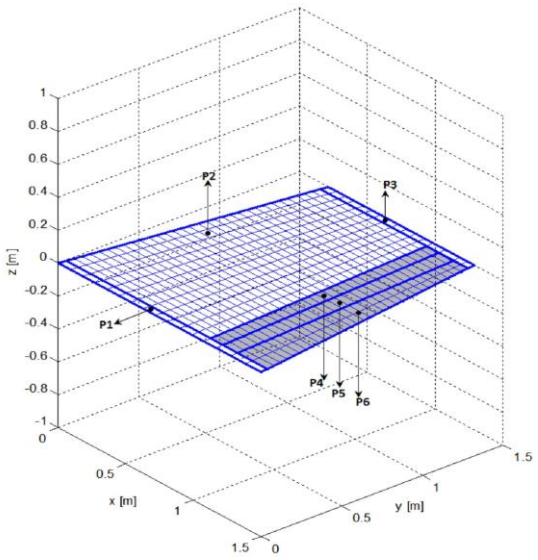

Figure 16. Test article (T/A) aerodynamic lattice.

IV. Aeroelastic Stability Analysis

Flutter analyses were carried out under the following assumptions (in compliance with applicable airworthiness requirements [14]):

- PK-continuation method with rationalization of generalized aerodynamic forces (GAF) for the evaluation of modal frequencies and damping trends versus flight speed;
- Theoretical elastic modes association in the frequency range 0Hz-80Hz (elastic modes being pertinent to T/A constraint expected during tests);
- Modal damping (conservatively) equal to 0.01 for all the elastic modes;
- See-level altitude, airspeed range 0-2*VM, with the maximum airflow speed expected during Wind Tunnel Tests VM=85 m/s.
- Morphing aileron actuators in power-on configuration (fixed value of rotational stiffness at internal aileron actuators' shafts).
- External actuator stiffness according to values reported in Table II.

In such a way, several aeroelastic stability analyses were performed in correspondence of different control surface harmonic covering a wide range of values for the stiffness of aileron (external) actuator summarized in Table II; this sensitivity analysis will be useful to demonstrate the robustness of the obtained results. In addition, for each stiffness value, modal frequency and damping trends versus airflow speed (i.e. V-g plots) were traced to detect potential dynamic instabilities (flutter).

Trends of modes frequencies and damping versus flight speed have been plotted in Fig. 17 and flutter analysis results summarized in Table IV. For all the investigated cases, flutter (*sharp type*) of mode 3 (aileron tab mode, see Fig. 11) was always detected at speed higher than $1.2*V_M$.

Accurate analysis of modes participation factors into flutter mode were performed in order to isolate the principal modes involved in each detected flutter.

For each case (Table II), in-depth analysis of flutter eigenvector participation factors was performed and minimum number of modes, involved in flutter instability, was detected (Fig. 18).

The aeroelastic instability was found to be essentially due to a typical ternary mechanism characterized by the coalescence of modes 1 (*aileron harmonic*, Fig. 11) and 3 (*aileron tab mode*, Fig. 13) sustained by mode 2 (*T/A bending* Fig. 12). As external linear actuator stiffness increases, frequency of the aileron harmonic gets closer to the one of the flutter mode (aileron tab mode fairly constant at 22 Hz). On the other hand, the trend of the flutter speed versus the parameter K (Fig. 19) shows an asymptotical stabilization at around 108 m/s for $K \rightarrow \infty$; this means that the flutter speed keeps to be greater than 1.2*VM also in correspondence of K values greater than the ones covered by the addressed analysis cases.

In addition, complete overview of the flutter speed trends versus the stiffness of the external linear actuator was obtained taking into account several modes association (as shown in Fig. 19). The trend shows that the critical flutter speed is sensitive to the *elastic coupling* between the wing model and the aileron [18], in addition

to the *aerodynamic coupling* (i.e. nonvanishing aerodynamic moment about the aileron hinge line [18]). Finally, results confirm that no aileron "dynamic mass balancing" was required to assure flutter clearance. All scheduled Wind Tunnel Tests were successfully performed [8]; accelerometers (installed on the wing box, and on the aileron) showed regular vibration behavior of the test article [8].

V. Conclusions

The authors intensively worked on the flutter clearance demonstration of the wind tunnel wing model equipped with a full-scale variable-camber aileron driven by load-bearing electro-mechanical actuators. Test article (T/A) aeroelastic stability analysis was a relevant assessment activity of CRIAQ MDO-505 project.

Due to the higher complexity of the system with respect to conventional solutions based on conventional aileron, it was believed necessary to demonstrate flutter clearance up to 1.2 times the maximum flow speed expected during Wind Tunnel Tests. Rational approaches were implemented in order to simulate the effects induced by variations of aileron actuator's stiffness on the aeroelastic behavior of the wing.

Reliable models were properly implemented to enable fast aeroelastic analyses covering several configuration cases in order to prove clearance from any dynamic instability (flutter) up to 1.2 times the maximum flow speed expected during Wind Tunnel Tests.

Flutter clearance of the T/A was justified by means of rational analysis based on theoretical modes association and implementing numerical methods and approaches consistent to the airworthiness requirements [14].

T/A was proven to be free from any dynamic instability up to 1.2 times the maximum airflow speed expected during test (85 m/s, [8]); the robustness of the obtained results was demonstrated with respect to changes in control surface harmonic covering a wide range of values for the stiffness of the aileron (external) actuator.

In-depth analysis results showed that the aeroelastic instability was due to a typical ternary mechanism characterized by the coalescence of aileron harmonic (Fig.11), and *aileron tab mode*, (Fig.13) sustained by T/A bending (mode 2, Fig. 12).

Finally, complete overview of the flutter speed trends versus the stiffness of the external linear actuator was obtained taking into account several modes association.

Such aeroelastic model and results may be properly taken in account for future assessment of morphing aileron device on EASA CS-25 category aircraft (i.e. concerning internal actuator failure or jamming, change in mass or stiffness of the actuation system).

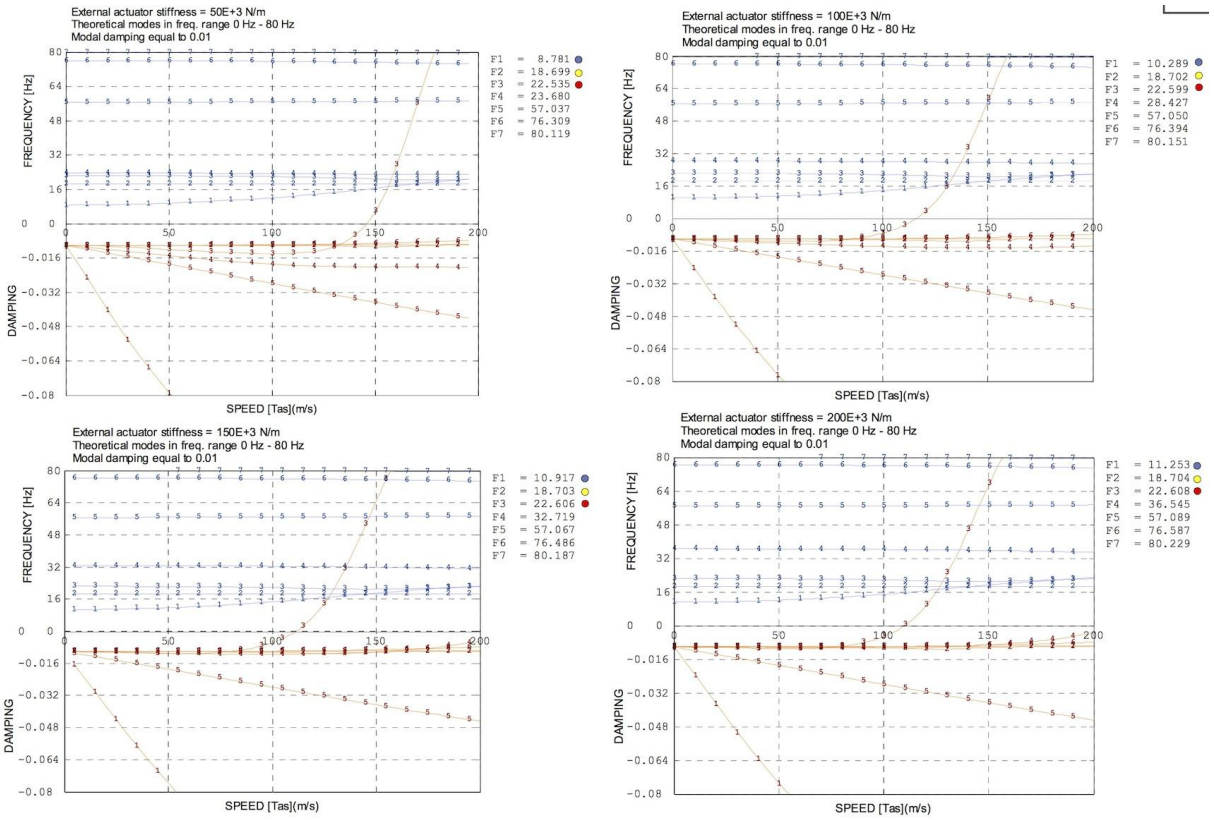

Figure 17. V-g plot.

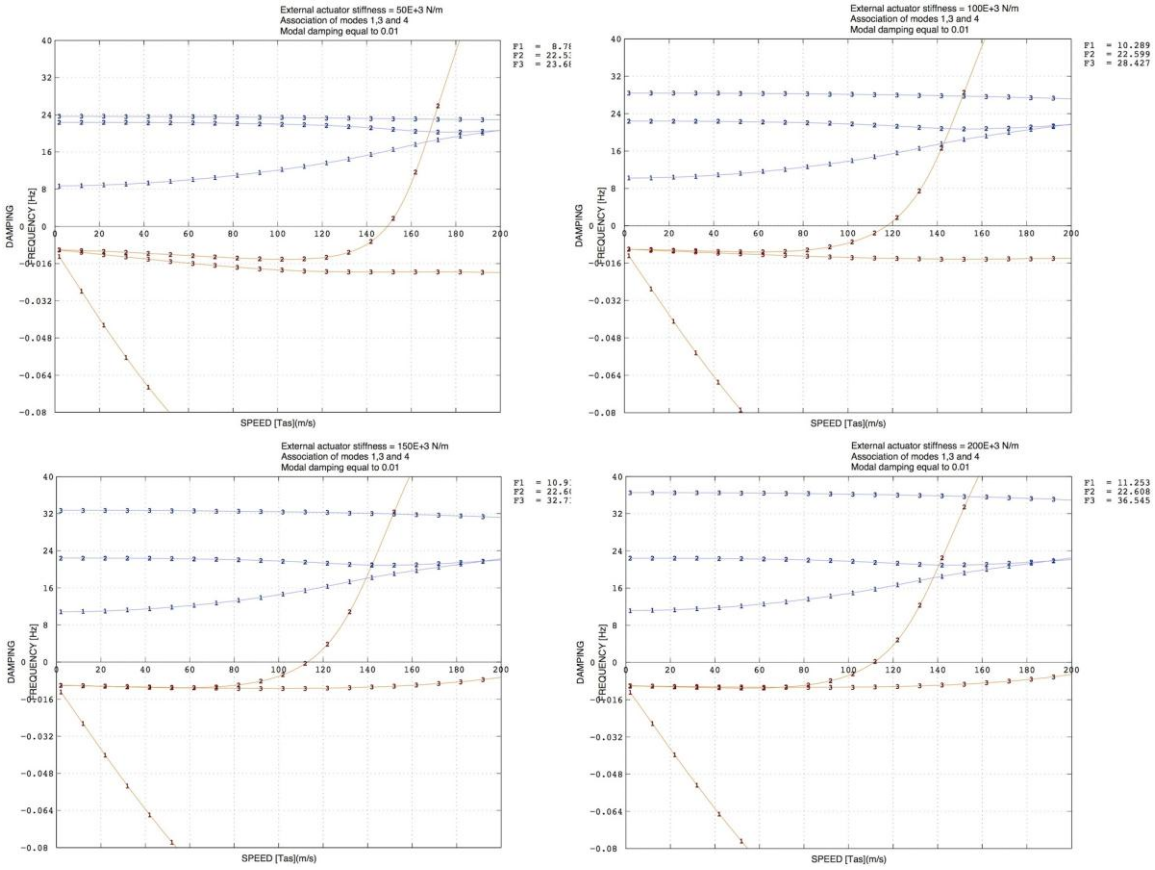

Figure 18. V-g plot: minimum number of modes (involved in flutter instability).

TABLE IV. FLUTTER ANALYSIS RESULTS.

CASE ID	K [N/m]	V_F [m/s]	V_F / V_M	FLUTTER MODE ID (frequency)
1	5.0 E+04	146.081	1.719	3 (22.53 Hz)
2	1.0 E+05	115.724	1.361	3 (22.59 Hz)
3	1.5 E+05	111.353	1.310	3 (22.60 Hz)
4	2.0 E+05	109.872	1.293	3 (22.60 Hz)

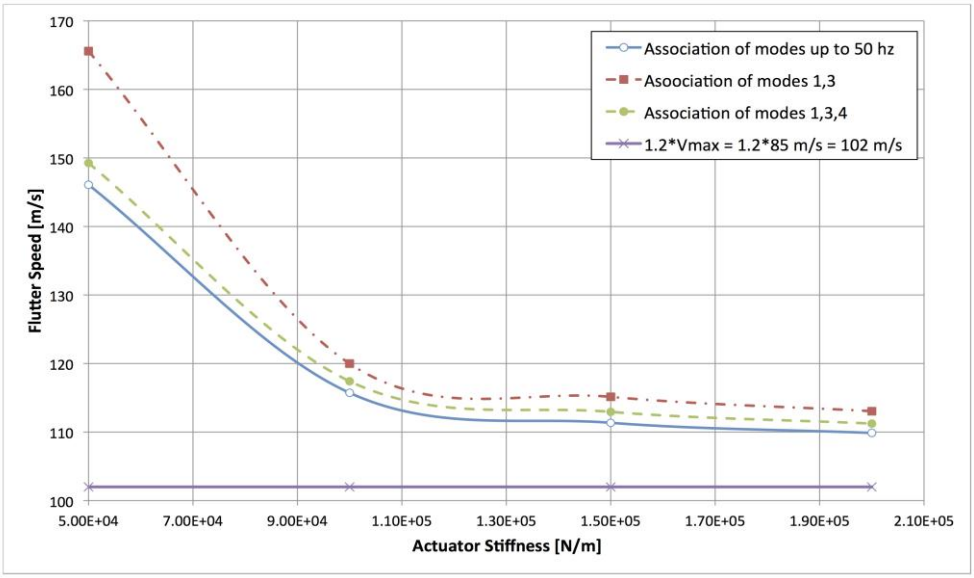

Figure 19. Flutter speed vs. aileron actuator stiffness.

APPENDIX A – SANDY 3.0 SOFTWARE GENERAL DESCRIPTION

SANDY is an in-house (currently not-commercial) code, which has been developed and upgraded within last twenty-five years with the intent of providing an excellent and reliable tool for static and dynamic aeroelastic and aero-servo-elastic analysis of aircraft.

Rational approaches and validated numerical methods, compliant with EASA standards CS-25 and CS-23, have been implemented in a multidisciplinary computational environment able to accomplish the following main tasks:

- Generation of aircraft dynamic model (structural model and inertial model);
- Generation of accurate transfer matrices interfacing between dynamic and aerodynamic models;
- Evaluation of aircraft acceleration and loads response due to flight and ground maneuver and/or gust;
- Evaluation of aircraft static and dynamic acceleration and loads response to movable lifting surfaces deflections imposed by mechanical and/or electro-mechanical control circuits;
- Evaluation of divergence, control reversal and flutter speeds.

The computational tool, and the numerical methods within implemented, assure fast analyses aimed also to investigate the influence of several design parameters on A/C aeroelastic behavior; in other terms, it is provided the capability of fast sensitivity aeroelastic analysis in correspondence of variations in structural and dynamic properties pertaining to A/C components including also the integrated control circuits.

Software overall facilities and performances have been positively tested during the certification processes of a wide set of commercial aircraft with reference to the aeroelastic stability demonstration at both theoretical and experimental levels (see as example [19], [20]).

ACKNOWLEDGMENT

The authors acknowledge ETS (L'École de Technologie Supérieure), NRC (Canadian National Research Council), CIRA (Centro Italiano Ricerche Aerospaziali), Bombardier Aerospace, Thales Aerospace and Finmeccanica Aircraft Division for their technical support as partners of the CRIAQ MDO-505 project.

REFERENCES

[1] S. V. Thornton, "Reduction of structural loads using maneuver load control on the advanced fighter technology integration (AFTI)/F-111 mission adaptive wing," *NASA Technical Memorandum 4526*, September 1993.
[2] S. Barbarino, O. Bilgen, R. M. Ajaj, M. I. Friswell, and D. J. Inman, "A review of morphing aircraft," *Journal of Intelligent Material Systems and Structures*, vol. 22, Aug. 2011, pp. 823-877.
[3] Saristu Project. Available at: http://www.saristu.eu
[4] F. Rea, M. Arena, M. C. Noviello, R. Pecora, and F. Amoroso, "Preliminary failure analysis of an innovative morphing flap tailored for large civil aircraft applications," in *Proc. 2016 7th International Conference of Mechanical and Aerospace Engineering*, ICMAE 2016, London, 18-20 July 2016, pp. 534-542.
[5] CRIAQ MDO-505 Project. Available: [Online]. http://en.etsmtl.ca/Unites-de-recherche/LARCASE/Recherche-et-innovation/Projects.
[6] E. Stanewsky, "Adaptive wing and flow control technology," *Progress in Aerospace Science*, vol. 37, Oct. 2001, pp. 583-667.
[7] R. Pecora, F. Amoroso, and L. Lecce, "Effectiveness of wing twist morphing in roll control," *Journal of Aircraft*, vol. 46, no. 6, pp. 1666-1674, 2012.
[8] R. M. Botez, A. Koreanschi, O. S. Gabor, Y. Mebarki, M. Mamou, Y. Tondji et al. "Innovative wing tip equipped with morphing aileron for greener aviation," in *Proc. the Conference Greener Aviation 2016*, Oct. 11-13, Brussels, Belgium.
[9] M. J. T. Kammegne, M. R. Botez, M. Mamou, Y. Mebarki, A. Koreanschi, O. S. Gabor, and T. L. Grigorie, "Experimental wind tunnel testing of a new multidisciplinary morphing wing model," in *Proc. the 18th International Conference on Mathematical Methods*, computational techniques and intelligent systems, MAMECTIS 2016.
[10] G. Amendola, I. Dimino, A. Concilio, F. Amoroso, and R. Pecora, "Preliminary design of an adaptive aileron for the next generation regional aircraft," *Journal of Theoretical and Applied Mechanics*, vol. 55, pp. 307-316.
[11] MSC/MD NASTRAN®, Software Packege, Ver. R3-2006, "Reference Manual".
[12] I. Dimino, D. Flauto, G. Diodati, A. Concilio, and R. Pecora, "Actuation system design for a morphing wing trailing edge," *Recent Patents on Mechanical Engineering*, vol. 7, 2014, pp. 138-148.
[13] G. Amendola, M. Magnifico, R. Pecora, and I. Dimino, "Distributed actuation concept for a morphing aileron device," *The Aeronautical Journal*, vol. 120, September 2016, pp. 1365-1385.
[14] European Aviation Safety Agency, "Certification specifications and acceptable means of compliance for large airplanes – CS-25," *Amendment 11*, July 11 2011, Subpart D, Pargraph 629.
[15] E. G. Broadbent, "Flutter and response calculations in practice," *AGARD Manual on Aeroelasticity*, vol. 3, NASA, 1963, p. 3, chap.4.
[16] MSC MD NASTRAN®, Software Package, Ver. R3-2006, "Quick Reference Guide".
[17] M. Arena, M. C. Noviello, F. Rea, F. Amoroso, R. Pecora, and G. Amendola, "Modal stability assessment for a morphing aileron subjected to actuation system failures," in *Proc. 2016 7th International Conference of Mechanical and Aerospace Engineering*, ICMAE 2016, London, 18-20 July 2016, pp. 437-442.
[18] Y. C. Fung, *An Introduction to the Theory of Aeroelasticity*, Dover Publications, 1993, pp. 172-174.
[19] R. Pecora, M. Pecora, and L. Lecce, "Flutter certification of SKYCAR aircraft: Rational analysis and flight tests," in *Proc. the 3rd CEAS Air&Space Conference*, Venice, Italy, September, 2011.
[20] R. Pecora, M. Magnifico, F. Amoroso, and E. Monaco, "Multi-parametric flutter analysis of a morphing wing trailing edge," *The Aeronautical Journal*, vol. 118, no. 1207, September 2014, pp. 1063-1078.

Francesco Rea, born in Naples (Italy) the 9th of August 1990, graduated with honors in Aerospace Engineering (MSc) the 5th of February 2015 with a master's thesis on the aero-servo-elastic behavior of a morphing aileron. He is currently a Ph.D. candidate in Industrial Engineering at the University of Naples "Federico II". He is actually working on the structural design of morphing high-lift devices (within the framework of CleanSky GRA, and CleanSky 2) in compliance with industrial standards and applicable airworthiness requirements: from preliminary structural layout to full-scale ground static testing. He is author of three scientific papers, presented at Conferences.

Rosario Pecora, Master degree in Aeronautical Engineering and Ph.D. in Transport Engineering awarded by the University of Naples "Federico II" on 2002 and 2005. Assistant Professor of Aircraft Structures Stability and Lecturer of Advanced Aircraft Structures at the same University since 2011. He has worked for many aircraft manufacturing companies (including but to limited to ATR, ALENIA AERMACCHI, BOMBARDIER, PIAGGIO AEROINDUSTRIES) and research centers as technical advisor for loads, aeroelasticity, aircraft structures design and certification (EASA CS-23,-25 standards). His research activity is mainly focused on aero-servo-elasticity of unconventional structural systems, structures dynamics and smart structures while covering leading roles in major European and extra-European projects (CAPECON, Clean Sky GRA, SARISTU, CRIAQ-MDO505, Cleans Sky 2). He is author of several scientific papers and designed inventor of European and US patents on SMA-based architectures for morphing wing trailing edge.

Francesco Amoroso, took his degree in Aerospace Engineering with honour at the University of Napoli "Federico II" (Italy) in 2004; there, he was also awarded with his PhD in Aerospace Engineering in 2009. Assistant Professor of Turbomachinery Structural Design and Lecturer of Advanced Aircraft Structures at the same University since 2011. He has worked for many companies (ALENIA AERMACCHI, AVIO SPA, PININFARINA) and research centers (CIRA, CNR, ONERA), as well as for European Academies (Trinity College of Dublin, Universität des Saarlandes - LPA). His research activity is focused on experimental aeroacoustics, structures dynamics and design of conventional and smart structures. He covered and currently covers leading roles in national and international research projects (MESEMA, COMFORT, SEFA, COSMA, CleanSky GRA, CleanSky 2); his researches have been published in nearly fifty contributes to conference proceedings and scientific journals.

Maurizio Arena, is attending a Ph.D. program in the Department of Industrial Engineering of University of Napoli "Federico II" (Italy) where he graduated with honour in Aerospace Engineering in 2015 with a thesis focused on the aero-servo-elastic stability assessment of a morphing trailing edge within the SARISTU European project. His research topics are directed toward the design and validation of smart systems for the next generation aircraft. In such context, several innovative solutions addressed at optimizing the aircraft weight and operative costs as well as an enhancement in the flight performance and internal comfort have been developed.

Maria Chiara Noviello, was born in Cerreto Sannita (BN) (Italy), on January 6th, 1991. She graduated with honors in Aerospace Engineering at the University of Naples "Federico II" with a master thesis about the experimental shape reconstruction of a morphing wing trailing edge prototype, achieved on April 7th, 2015. She is currently a Ph. D. candidate in Industrial Engineering. In her research, she investigates aeroelastic trade-off analyses of adaptive trailing edge devices for wing load control. Recent activities regard the control system design for a morphing wing flap demonstrator. She is author of three scientific papers presented at conferences.

Gianluca Amendola, Master degree in Aerospace Engineering with honor at the University of Napoli "Federico II" (Italy) in 2012. Since 2014, he is a Researcher at the Department of Smart Structures of the Italian Aerospace Research Centre (CIRA). Actually he is working in the Clean Sky 2 (Airgreen) WP 2.1.2 for the design of a morphing winglet for flight tests. In 2016, he successful completed PhD at University of Naples in the framework of CRIAQ MD0505 project. His research regards the design, manufacturing and testing of a morphing aileron for next-generation regional aircraft.